

CALCULATING VACUUM ENERGIES IN QUANTUM FIELD THEORY

MARKUS QUANDT

*Institute for Theoretical Physics
University of Tübingen
D-72076 Tübingen, Germany*

A new approach to generalised Casimir type of problems is derived within the context of renormalisable quantum field theory (QFT). We study the simplest case of a massive fluctuating boson field coupled to a time-independent background potential. We use analytic properties of scattering data to compute the relevant Green's functions at imaginary momenta, which in turn yields a simple and efficient method to compute (one-loop) vacuum energy densities in QFT. Renormalisation is easily performed in the perturbative sector by identifying low order Feynman diagrams with the first few Born approximation to the Green's function. Numerical examples illustrate the efficiency of our approach.

1 Introduction

In this talk, I report on the technical aspects of a novel quantum field theory approach to generalised Casimir problems. The work presented here was done in collaboration with N. Graham, R. L. Jaffe, V. Khemani, M. Scandurra, O. Schröder and H. Weigel; for a more complete exposition, see ref.¹.

The traditional approach to Casimir systems imposes boundary conditions on a quantum field *ab initio*². In reality, however, Casimir forces arise from *interactions* between the quantum field and matter, and no such interaction is strong enough to enforce a boundary condition on *all* frequencies of the fluctuating field. To study whether an idealised boundary condition limit exists in which physical quantities become independent of the regularisations involved, we have recently proposed³ to embed the Casimir calculation in a quantum field theory (QFT). The external condition is then replaced by a renormalisable interaction with a smooth background field that imposes the boundary condition in a certain limit. QFT renormalisation is the only sensible way to discuss and eventually remove UV divergences. Any remaining infinities in our approach indicate that the quantities under consideration depend in detail on the physical UV cutoff provided by the material. In ref.⁴ we argued that the traditional approach is perfectly valid for some quantities (e.g. forces between rigid bodies) while it fails for others (e.g. the Casimir stress on isolated surfaces).

Since the boundary condition limit in the QFT approach involves arbitrarily strong and sharply peaked background fields, the standard tools for the calculation of effective energies (or functional determinants) cannot be employed: Perturbation theory fails because of the strong coupling, while a derivative expansion is ruled out by the high Fourier modes in the background

field. Thus, we had to develop general new methods to compute renormalized one-loop quantum energies and energy densities.^a These methods are important in their own right and have a much broader application than the proper Casimir problem studied in ref.⁴; for details the reader is referred to refs.⁶. In the present talk, I will concentrate on the derivation of our approach from conventional quantum field theory, which is presented in section 2. Computational techniques for Green's functions and renormalisation are discussed in section 3. Section 4 presents a numerical example to demonstrate the efficiency of our method. I conclude with a brief summary and outlook on future directions.

2 The Method

For simplicity, I will restrict myself to the case of a massive scalar boson ϕ interacting with a time-independent scalar background field $\sigma(\mathbf{x})$ through the coupling $\mathcal{L}_{\text{int}} = -\frac{\lambda}{2}\phi^2\sigma(\mathbf{x})$. This model is renormalisable (in $n \leq 3$ space dimensions) and can be used as a QFT implementation of *Dirichlet b.c.* on a surface \mathcal{S} ,⁴ if we let the background σ be strong and sharply concentrated on \mathcal{S} . In general, our method requires that the background is sufficiently short ranged so that a conventional scattering theory can be defined. More importantly, we require enough (spherical) symmetry to separate the scattering problem into partial waves; we shall consequently assume that $\sigma(\mathbf{x})$ only depends on $r = |\mathbf{x}|$. The vacuum energy density in a spherical shell of radius r is then

$$\epsilon(r) \equiv \frac{2\pi^{n/2}}{\Gamma(n/2)} r^{n-1} \left\langle \Omega \left| \frac{1}{2} [\dot{\phi}^2 + (\nabla\phi)^2 + m^2\phi^2 + \sigma(r)\phi^2] \right| \Omega \right\rangle_{\text{ren}} \quad (1)$$

where $|\Omega\rangle$ is the interacting vacuum and the operator in the vev is just the symmetric energy density operator \hat{T}_{00} for our model. To further evaluate eq. (1), we first perform a partial wave decomposition of the field operator, $\phi(t, \mathbf{x}) = \sum_{\{\ell\}} \phi_{\ell}(t, r) \mathcal{Y}_{\{\ell\}}(\hat{x})$ where $\mathcal{Y}_{\{\ell\}}(\hat{x})$ are the n -dimensional spherical harmonics and $\{\ell\}$ refers to the set of all angular quantum numbers in n space dimensions. Finally, we make a *Fock decomposition* for the radial operators,

$$\phi_{\ell}(t, r) = r^{\frac{1-n}{2}} \int_0^{\infty} \frac{dk}{\sqrt{\pi\omega}} \left[\psi_{\ell}(k, r) e^{-i\omega t} a_{\ell}(k) + \psi_{\ell}^*(k, r) e^{i\omega t} a_{\ell}^{\dagger}(k) \right] + \text{b.s.} \quad (2)$$

with $\omega = \sqrt{m^2 + k^2}$. The wave functions $\psi_{\ell}(k, r)$ in eq. (2) are a complete set of scattering and bound state^b solutions to the fully interacting field equa-

^aIt should be mentioned that the *world-line formalism*⁷ provides an alternative way for an exact (numerical) computation of 1-loop quantum energies. It is even applicable in cases where there is not enough radial symmetry for our method to work.

^bThe term "b.s." in eq. (2) indicates a similar contribution from the bound states of energy $\omega_j = \sqrt{m^2 - \kappa_j^2}$, which are required for the completeness of the function system.

tions. They can be ortho-normalised such that the expansion coefficients $a_\ell(k)$ obey the standard commutation relations $[a_\ell(k), a_{\ell'}^\dagger(k')] = \delta(k - k')\delta_{\ell\ell'}$, (and similarly for the b.s.) which allows the usual particle interpretation (e.g. $a_\ell^\dagger(k)$ creates a ψ_ℓ -mode acting on $|\Omega\rangle$).

Inserting our decomposition back into eq. (1), the result is best expressed in terms of the *Green's function*

$$G_\ell(r, r'; k) = -\frac{2}{\pi} \int_0^\infty dq \frac{\psi_\ell^*(q, r)\psi_\ell(q, r')}{(k + ie)^2 - q^2} - \sum_j \frac{\psi_{\ell,j}(r)\psi_{\ell,j}(r')}{k^2 + \kappa_j^2} \quad (3)$$

which is meromorphic in the upper complex k -plane with simple poles at the bound state momenta $k = i\kappa_j$ (in the next section, I will sketch an efficient method to compute G_ℓ). The Green's function is intimately related to the density of states. In fact, defining a *local spectral density*

$$\rho_\ell(k, r) \equiv -ik G_\ell(r, r; k), \quad \text{Im } k \geq 0 \quad (4)$$

in the upper k -plane, we easily recover the local density of states for real k ,

$$\text{Re } \rho_\ell(k, r) = \text{Im } \{k G_\ell(r, r; k)\} = \psi_\ell^*(k, r)\psi_\ell(k, r).$$

The energy density, eq. (1), can be expressed (up to a total derivative) as an integral of the single particle energies $\omega(k)$ over all real k , weighted by the local density of states in each channel ℓ (plus a contribution from the bound states ω_j). For practical purposes, however, it is much more convenient to rotate the integration contour to the upper complex k -plane. We get three contributions: (1) The residues from the bound state poles on the imaginary axis cancel the explicit bound state contribution in G_ℓ exactly,⁵ (2) the discontinuity of the square root cut in the single particle scattering energies $\omega = \sqrt{m^2 + k^2}$ yields an integral along the imaginary axis, $k = it$, $t \in [m, \infty]$, and (3) the big semicircle at infinity gives no contribution if the integrand falls off fast enough for $|k| \rightarrow \infty$. To ensure (3), we have to improve the decay of the local spectral density eq. (4) at large $|k|$. Since the *Born series* to the Green's function converges at large $|k|$, it is sufficient to subtract a few low order Born approximations. We use the notation

$$[\rho_\ell(k, r)]_N \equiv \rho_\ell(k, r) - \rho_\ell^{(0)}(k, r) - \cdots - \rho_\ell^{(N)}(k, r) \quad (5)$$

for the N times Born subtracted density (and similarly for the Greens function). Formally, the Born series is an expansion of G_ℓ in powers of the interaction, i.e. the coupling strength λ . When used in the expression for the energy density $\epsilon(r)$, the Born terms should thus correspond to the usual perturbative *Feynman series*. Notice that we need a cutoff at this point since the low order Feynman diagrams and Born approximations to G_ℓ are precisely the UV divergent parts of the calculation. Using dimensional regularisation, the identification of Born and Feynman series has been established rigorously

at least for the lowest orders⁶. The final result for the energy density in a spherical shell of radius r is then^c

$$\begin{aligned}\epsilon(r) = & -\sum_{\ell} N_{\ell} \int_m^{\infty} \frac{dt}{\pi} \sqrt{t^2 - m^2} \left[1 - \frac{1}{4(t^2 - m^2)} D_r \right] [\rho_{\ell}(it, r)]_N + \\ & + \sum_{i=1}^N \epsilon_{\text{FD}}^{(i)} + \epsilon_{\text{CT}}(r).\end{aligned}\quad (6)$$

Here, N_{ℓ} is the multiplicity in the channel ℓ , $D_r = \partial_r(\partial_r - (n-1)/r)$ is a total derivative operator and ϵ_{CT} denotes the *counter terms* necessary to renormalise the N low order Feynman diagrams $\epsilon_{\text{FD}}^{(i)}$. The perturbative renormalisation of ϵ_{FD} is standard and briefly sketched in the next section, where I also present an efficient method to evaluate the local density ρ_{ℓ} and its Born series. It should be emphasised that eq. (6) yields a finite renormalised vacuum energy density for any smooth background $\sigma(r)$. Renormalisation group arguments prove that the final result is cutoff- and scheme-independent.

To compute the *quantum energy* $E_q[\sigma]$ we can simply integrate eq. (6) over all radii. Using the formula¹

$$2 \int_0^{\infty} dr [\rho_{\ell}(k, r)]_0 = i \frac{d}{dk} \ln F_{\ell}(k) \quad (7)$$

valid in the upper complex k -plane, we can relate the density of states in k -space to the log-derivative of the *Jost function* $F_{\ell}(k)$. Rotating back to the real axis from above, this turns into the well-known expression

$$[\rho_{\ell}(k)]_0 = \rho_{\ell}(k) - \rho_{\ell}^{(0)}(k) = \frac{1}{\pi} \frac{d\delta_{\ell}}{dk} \quad (8)$$

for the (change in the) density of states in terms of the *phase shift* δ_{ℓ} . Thus we have the quantum energy (\equiv change in the zero-point energy due to the background σ)

$$E_q[\sigma] = \sum_{\ell} N_{\ell} \int_m^{\infty} \frac{dt}{2\pi} \frac{t}{\sqrt{t^2 - m^2}} [\nu_{\ell}(t)]_N + \sum_{i=1}^N E_{\text{FD}}^{(i)} + E_{\text{CT}} \quad (9)$$

where $\nu_{\ell}(t) = \ln F_{\ell}(it)$ is the log of the Jost function on the imaginary axis.

The continuation of eq. (9) back to the real axis has been used extensively in the past⁶. Though eq. (9) is superior from a computational point of view, the formula on the real axis has the merit of a clear physical interpretation in terms of one-particle states and densities. In the next section, I will briefly discuss the methods necessary to turn eq. (6) and (9) into efficient computational tools.

^cSince the vacuum bubble diagram $\epsilon_{\text{FD}}^{(0)}$ is not inserted back, eq. (6) really represents the *change* in the vacuum energy due to the interaction.

3 Computational Techniques and Renormalisation

The Feynman series for the energy density is obtained from the usual perturbative expansion^d

$$\langle 0 | \hat{T}_{00}(x) | 0 \rangle = \frac{1}{2i} \text{Tr} \left[\hat{T}_x (-\partial^2 - m^2 - \sigma)^{-1} \right] \quad (10)$$

where \hat{T}_x is the coordinate space operator corresponding to the insertion of the energy density (1) at the space-time point x . It has pieces of order σ^0 and σ^1 which read, in momentum space,

$$\begin{aligned} \langle k' | \hat{T}_x^{(0)} | k \rangle &= e^{i(k'-k)x} [k'^0 k^0 + \mathbf{k}' \cdot \mathbf{k} + m^2] \\ \langle k' | \hat{T}_x^{(1)} | k \rangle &= \sigma(x) e^{i(k'-k)x}. \end{aligned} \quad (11)$$

The Feynman series consists of all graphs with a single ϕ -loop and arbitrary insertions of $\hat{T}_x^{(0)}$, $\hat{T}_x^{(1)}$ and $\sigma(x)$ (from expanding the propagator in eq. (10)). To order σ^1 , for instance, we have two diagrams: (a) a single insertion of $\hat{T}_x^{(1)}$ and (b) one insertion of σ and one insertion of $\hat{T}_x^{(0)}$. Only diagram (a) (the *tadpole graph*) is divergent,

$$\frac{1}{2i} \text{Tr} \left[\hat{T}_x^{(1)} (-\partial^2 - m^2)^{-1} \right] = \frac{i}{2} \sigma(\mathbf{x}) \int \frac{d^d k}{(2\pi)^d} \frac{1}{k^2 - m^2}. \quad (12)$$

It may easily be renormalised (and even cancelled completely) by a counter term proportional to $\sigma(\mathbf{x})$. For the present model the tadpole counter term $c_1 \sigma$ and one Born subtraction $N = 1$ are in fact sufficient for space dimension up to $n = 2$. In $n = 3$, an additional mass counter term $c_2 \sigma^2$ is required and we have to perform $N = 2$ Born subtractions. The coefficient c_2 may be fixed by a specific choice of renormalisation condition but the renormalisation group ensures that physical quantities are scheme independent.

More generally, the counter terms are *local monomials* in σ and $\partial\sigma$. It is then immediately clear that renormalisation will only affect the energy density on the *support* of the counter terms. For a Casimir type of calculation, the background becomes sharply concentrated on the b.c. surfaces and the energy density away from the surfaces cannot be affected by the counterterms; it must thus be finite. The divergence of the energy density as one approaches Casimir surfaces has in fact been known for a long time.⁸

The final ingredient in our main formula, eq. (6), is the appropriate Green's function, which may be expressed as a product of Jost (f_ℓ) and regular (ϕ_ℓ) solution to the scattering problem,

$$G_\ell(r, r'; k) = (-k)^{\ell+(n-3)/2} \frac{\phi_\ell(k, r_<) f_\ell(k, r_>)}{F_\ell(k)}.$$

^dFor the total energy eq. (9), the Feynman diagrams are more easily computed from the functional determinant representation $E_q = \frac{1}{2T} \ln \det(-\square + m^2 + \sigma)$ in euclidean space (T is the euclidean time interval).

In order to evaluate this formula on the imaginary k -axis, it is important to cancel all oscillating pieces in the numerator, which would otherwise become numerically intractable in the upper complex k -plane. We cancel the free Jost solution $w_\ell(kr)$ (a modified Hankel function) explicitly by the ansatz $f_\ell = w_\ell g_\ell$ and $\phi_\ell \sim h_\ell/w_\ell$. The result is a representation of the form^e

$$G_\ell(r, r; k) = \frac{h_\ell(k, r)g_\ell(k, r)}{(2\ell - 2 + n)g_\ell(k, 0)} \quad (13)$$

in terms of two new functions g_ℓ and h_ℓ . Since both the Jost and regular solution obey the full radial field equation with certain boundary conditions, it is easy to derive ODE's for the relevant functions g_ℓ and h_ℓ . The explicit expressions are somewhat lengthy and the reader is referred to ref.¹ for details. A few general remarks are in order. By introducing *two* functions with boundary conditions at $r = 0$ (for h_ℓ) and at $r = \infty$ (for g_ℓ) we can avoid expensive shooting methods for the Green's function G_ℓ . The solutions g_ℓ and h_ℓ can be shown to be smooth *bounded* functions of r in the upper complex k -plane. The ODEs may, in fact, be solved directly on the imaginary axis $k = it$, where the solutions are *real* and easily amenable to numerical computations. The Born approximations are most conveniently computed by iterating the ODEs for g_ℓ and h_ℓ according to an expansion of G_ℓ in powers of the interaction σ .

Finally, a similar ansatz known as the *variable phase approach* can be used for the log of the Jost function required in the quantum energy formula, eq. (9). Writing $g_\ell(it, r) = e^{\beta_\ell(t, r)}$ with a *real* function β_ℓ , we find the relevant function $\nu_\ell(t) \equiv \beta(t, 0)$ by integrating the ODE

$$-\beta_\ell''(t, r) - [\beta_\ell'(t, r)]^2 + 2t\xi_\ell(tr)\beta_\ell'(t, r) + \sigma(r) = 0 \quad (14)$$

inwards, starting at $r \rightarrow \infty$ with $\beta_\ell(t, r) = \beta_\ell'(t, r) = 0$ (Born approximations follow again by iteration). The coefficient function ξ_ℓ is just the log-derivative of the free Jost function evaluated on the imaginary axis; for details see ref.¹.

4 A Numerical Example

As a numerical example for the efficiency of our method, I discuss a background field $\sigma(r)$ which takes the profile of a Gaussian ring in $n = 2$ space dimensions, $\sigma(r) = A \exp[-\frac{(r-a)^2}{2w^2}]$. In the limit where the width w tends to zero (and the strength to infinity) this background can be used to study the Casimir stress on a Dirichlet circle in $n = 2$ dimensions. Here, I will employ it as a numerical example of how our method handles sharply peaked backgrounds.

The left panel of figure 1 shows the contributions of various angular momentum channels to the quantum energy density. These terms correspond

^eThe *s*-wave in $n = 2, 3$ requires a slightly different treatment¹.

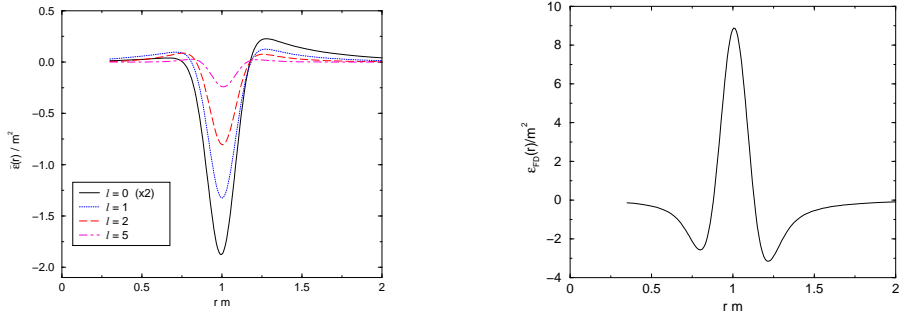


Figure 1. Left panel: Contributions of various angular momentum channels to the quantum energy density of the Gaussian ring. The first order Feynman diagram depicted in the right panel of fig. 1. From the scales at the axes, it is clear that the first order diagram dominates the energy density (i.e. perturbation theory is accurate) even at relatively large couplings (fig. 1 corresponds to $\lambda/m = 3.0$).

to the once Born subtracted t -integral in eq. (6), i.e. they do not include the 1st order Feynman diagram^f depicted in the right panel of fig. 1. From the scales at the axes, it is clear that the first order diagram dominates the energy density (i.e. perturbation theory is accurate) even at relatively large couplings (fig. 1 corresponds to $\lambda/m = 3.0$).

Figure 2 shows the complete quantum energy for Gaussian circles of various widths w . As can be seen from the height of the central peak, the density *on the surface* diverges in the sharp limit $w \rightarrow 0$ even after renormalisation. Our method allows to study this limit numerically by going to very small widths for which traditional approximation schemes fail.

5 Conclusion

In this talk, I have presented a new approach to the computation of 1-loop vacuum energies and energy densities in quantum field theory. Starting from a conventional Fock decomposition or, alternatively, from a Green's function approach, we identify the potential UV divergent contributions to the quantum energy with the low order Born approximations to the Green's function. We subtract these contributions and add them back as Feynman diagrams which allows for a conventional and scheme independent renormalisation using standard counter terms. The resulting formulae for the Casimir energy (density) are finite functionals of smooth background fields and easily amenable to numerical treatment. As an example, I have shown results for the Casimir energy density of a Gaussian circle in $n = 2$ space dimensions.

Our method has many interesting applications. Among the topics currently under investigation are magnetic vortices (which play a role in the

^fNote that the tadpole diagram has been cancelled completely by the counterterm, but there is still a second (finite) contribution of order σ^1 as explained in the last section.

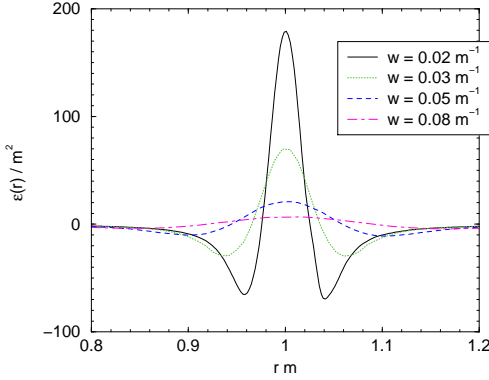


Figure 2. Quantum energy density for Gaussian rings of various widths w .

confinement properties of gauge theories) and Z -strings in electroweak theory, which bind fermions efficiently and may thus be of relevance in scenarios of baryogenesis.

References

1. N. Graham, R.L. Jaffe, V. Khemani, M. Quandt, M. Scandurra, H. Weigel, *Nucl. Phys. B* **645**, 49 (2002).
2. V. M. Mostepanenko and N. N. Trunov, *The Casimir Effect and its Application*, Clarendon Press, Oxford (1997);
K. A. Milton, *The Casimir Effect: Physical Manifestations of Zero-point Energy*, River Edge (USA): World Scientific (2001).
3. M. Bordag, U. Mohideen, V. Mostepanenko, *Phys. Rep.* **353** 1 (2001).
4. N. Graham, R.L. Jaffe, V. Khemani, M. Quandt, M. Scandurra, H. Weigel, *Phys. Lett. B* **572**, 196 (2003).
5. N. Graham, R.L. Jaffe, V. Khemani, M. Quandt, O. Schroeder, H. Weigel, *Nucl. Phys. B* **665**, 623 (2003).
6. M. Bordag, *J. Phys. A* **28** 755 (1995).
7. N. Graham, R. L. Jaffe, H. Weigel, *J. Mod. Phys. A* **17** (2002) and references therein;
E. Farhi, N. Graham, V. Khemani, R. L. Jaffe, H. Weigel, *Nucl. Phys. B* **630**, 241 (2002);
K. D. Olum and N. Graham, *Phys. Rev. D* **67**, 085014 (2003).
8. H. Gies, K. Langfeld, *Nucl. Phys. B* **613**, 353 (2001).
9. P. Candelas, *Ann. Phys.* **167** 257 (1986).